PRIMA

Small or medium-scale focused research project

SEVENTH FRAMEWORK PROGRAMME

THEME FP7-ICT-2009-4

INFORMATION SOCIETY TECHNOLOGIES

Deliverable 1.7 – Report on development and testing of three-dimensional model systems

Dissemination level: public

Contract no.:	248154
Project acronym:	PRIMA
Project full title:	Plasmon Resonance for IMproving the Absorption of solar cells
Project website:	http://www.prima-ict.eu

Coordinator contact details: Barry P. Rand (rand@imec.be)
IMEC
Kapeldreef 75
B-3001 Heverlee
Belgium
Tel: +32-16-287780
Fax:+32-16-281097

Document revision history

Version	Date	Author	Summary of main changes
0.1	29-06-2012	Vladimir Miljkovic	First version
0.2	08-02-2013	Vincenzo Giannini	Addition of III-V contribution

Table of Contents:

1 3D ‘stacked’ nanodisks on a-Si

As suggested in deliverable D1.7 we have investigated a possibility to incorporate a 3D geometry for enhancement of light scattering into the active layer of the solar cells. Inset in Fig. 1 shows one such example where two nanodisks on top of each other are used as a back reflector to enhance light scattering into the active layer (in this case for example an amorphous silicon aSi) of the solar cell. This modeled structure is one step forward in extending the functionality of HCL 2D structures above the substrate plane. In addition to this, we have calculated the scattering profiles for this structure.

A plane wave polarized along x-axis hits the aSi-glass interface under the normal incidence from aSi side. As short wavelengths are already absorbed inside the active layer, we designed our back reflector so that long wavelengths are effectively scattered into the active layer. In a typical aSi solar cell the efficiency of collecting carriers drops significantly after 700 nm, which makes an upper limit in wavelengths for light that we want to scatter with our device [1]. Therefore, we use two silver nanodisks, one small D60 with a diameter D = 60 nm and thickness t = 20 nm and one larger D80 with diameter D = 80 nm and thickness t = 20 nm. D60 is kept at a fixed position, i.e. 10 nm above aSi-glass interface, while position d of D80 disk was adjustable.

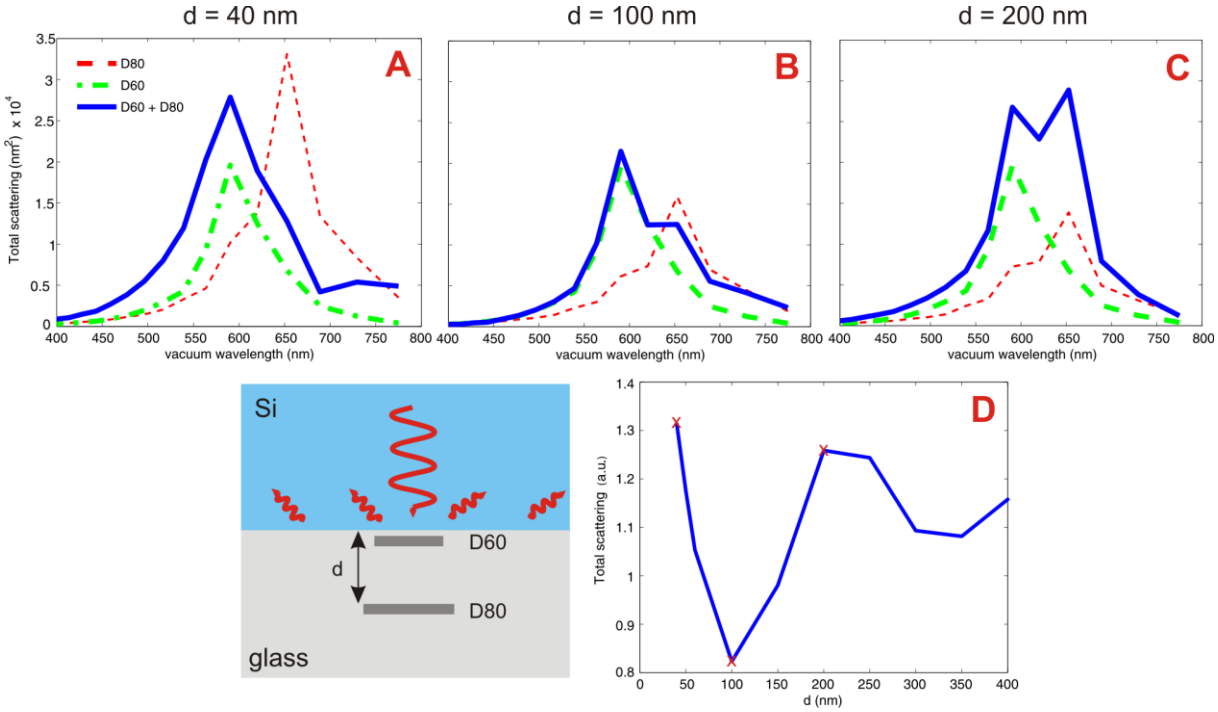

Figure 1. (inset) A plane wave incident from aSi side illuminates two Ag nanodisks positioned in glass, with thickness 20 nm and diameters 60 nm (D60) and 80 nm (D80) in a typical end-fire configuration. The larger disk is positioned on a distance d from the interface, while smaller disk is kept at a constant 10 nm distance from aSi-glass interface. (A-C) Total scattering into aSi for D60 (green dashed line), D80 (red dashed line) and both D60 and D80 (blue solid line) for different distances d. (D) Spectrally integrated total scattering into aSi for different distances d.

Fig. 1 (A-C) show the total scattering cross sections into aSi for three different distances d of the larger particle D80 (blue solid lines). In addition, we show the total scattering into aSi for D60 (green dashed lines) and D80 (red dashed lines) particles only. It is obvious that the scattering is

enhanced for the case when two particles are used as a back reflector compared to single particle cases. In addition, Fig. 1 (D) shows the spectrally integrated total scattering into aSi from 400 nm to 770 nm for different distance d. Clearly there is an optimal distance between the particles for which our 3D back reflector sends the most of light into the active layer.

As is well known, a point dipole source positioned at an interface of two medium will mostly radiate into a denser medium (in our case aSi), with a maximal radiation when it is positioned close to the denser refractive index medium [2, 3]. This is confirmed in our simulations as well (see red dashed line in Fig. 1(A-C)). This is a reason why we have decided to put D60 particle very close to the active layer. In order to further enhance the scattering of longer wavelengths we take a larger nanodisk D80 and put it right behind D60 on a distance d from the interface. In this way a shielding effect is avoided as well, which would happen if the bigger particle was positioned in the front of smaller one. However, it is clear from Fig. 1 (D) that there are few distances that can be chosen as optimal for enhancing the scattering into aSi layer.

The maximal scattering into the active layer happens when the particle D80 is positioned very close (d = 40 nm) to the particle D60. In this case a hybridized Fano type of resonance appears due to a strong interaction between the particles and the end-fire type of illumination (see references [4] for more detail). Namely, due to increased near fields at the particle D60 we get much more light out-coupled and scattered into the aSi layer. It is clear that this configuration enhances the scattering into aSi at wavelengths corresponding to the resonance of small particle D60 and not so much at longer wavelengths.

The other way to enhance the light scattered into the active layer would be by putting the particle D80 at d = 200 nm above the interface (see Fig. 1D). In this case (Fig. 1C), the total scattering spectra maintains two resonance peaks of both particles, but clearly much enhanced compared to the single particle spectra. The enhanced total scattering spectra is a result of constructive interference of light scattered from two particles separately. Clearly, this configuration provides an enhancement in scattering into aSi for longer wavelengths as is wanted.

Finally, if the particle D80 is positioned at d = 100 nm from the interface we get the total scattering into aSi that is still larger than from the individual particles, but smaller than in the previous two cases (d = 40 nm and 200 nm). The reason for this decrease in the total scattering is mainly due to destructive interference between the individual particle dipole moments when positioned at this particular distance d.

In addition to the investigation of spectral properties of 3D back reflector structure, the scattering profiles have been investigated as well. Fig. 2 (A-C) show the polar plots and Fourier images calculated at 570nm for three specific distances d = 40, 100 and 200 nm. The upper part of polar plots show the scattering into aSi, while bottom part represents scattering into glass, which is clearly much weaker. Fourier images represent scattering into aSi layer in the so-called Fourier plane k_x-k_y, where $k_x = k_{Si} \sin(\theta) \cos(\varphi)$, $k_y = k_{Si} \sin(\theta) \sin(\varphi)$ and $k_{Si} = 2\pi n / \lambda$ is wave number in aSi, with n refractive index of aSi and λ the free-space wavelength. The inner, dashed green circle is the border ($k_{||} = k_{glass}$) between propagating and evanescent waves in glass, while the solid green circle marks the same border ($k_{||} = k_{Si}$) for waves in the aSi. We mark the region $k_{||} < k_{glass}$ as the "allowed" and the region $k_{glass} < k_{||} < k_{Si}$ as the "forbidden" one.

Comparing the cases where there is maximum scattering into the active layer (Fig. 2 A and C), we see that the radiation profiles are quite different. As already mentioned the near field at the particle

D60 is substantially enhanced for d = 40 nm, which enhances the part of light scattered into the "forbidden" zone. The light scattered above the critical angle (22 degrees) can contribute to the guiding modes inside aSi, which is clearly an advantage of this configuration. On the other hand, for d = 200 nm, the most of light is scattered inside the "allowed" zone and evenly distributed inside it as a result of constructive interference between light scattered from both particles. Finally, at d = 100 nm light is more or less evenly distributed inside both "forbidden" and "allowed" zones, but clearly this is due to a decrease in light scattered in the "allowed" zone due to the destructive interference.

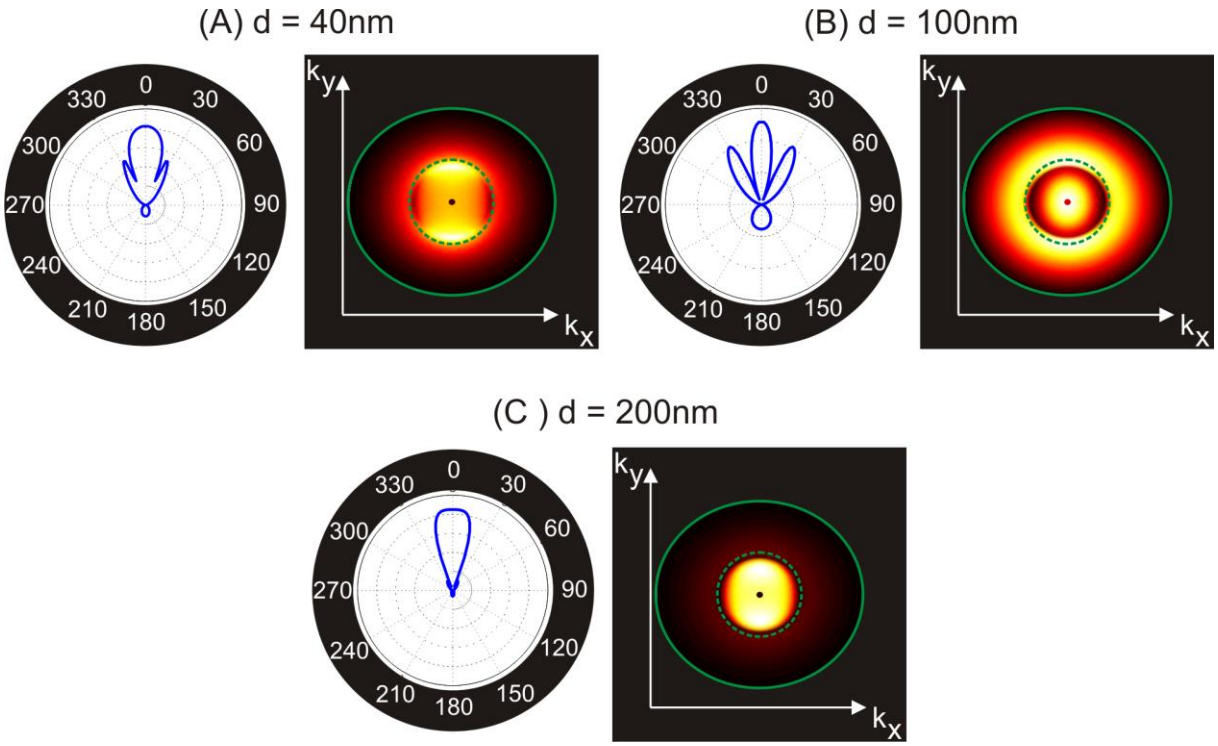

Figure 2. (A-C) Polar plots and Fourier images for different distances d calculated at a vacuum wavelength of 570 nm.

2 Conclusions

In conclusion, we have seen that the best performance of 3D back reflector would be if the particle D80 is positioned very close to the particle D60 or if it is positioned at a specific distance from it so that we have a constructive interference between dipoles excited in both particles. The former configuration has an advantage of enhancing the wave-guiding mode inside the active layer at wavelength corresponding to the resonance of particle close to the interface. On the other hand, the later configuration is very favorable for broadening the spectral range of light scattered into the active layer.

In addition we have seen that the best performances (theory and experiment) for plasmonic photodiode are obtained with Aluminum nano-cylinders with a pitch around 300-400 nm. With this parameters the EQE overcome the references for all the frequencies studied. Also it is important to highlight that 3D theoretical model we built gives very accurate predictions despite the complexity of the plasmonic solar cell structure. This is a key point in order to further optimize these kind of structures or explore new materials.

3 Methods

The calculations are done using the Green function method [5, 6]. Refractive index of glass used in the calculations is n_g = 1.5, while dielectric function of silver and aSi are taken from Johnson and Christy [7] and Palik [8], respectively.

4 References

[1] M. G. Deceglie, V. E. Ferry, A. P. Alivisatos, and H. A. Atwater, *Nano Letters*, **12**, 2894-2900 (**2012**).
[2] W. Lukosz, and R. E. Kunz, *J. Of Opt. Soc. Of Am.*, **67**, 1607-1615 (**1977**).
[3] W. Lukosz, and R. E. Kunz, *J. Of Opt. Soc. Of Am.*, **67**, 1615-1619 (**1977**).
[4] A. Dmitriev, T. Pakizeh, M. Käll, D. S. Sutherland, Small, **3**, 294-299 (**2007**).
[5] P. Johansson, *Phys. Rev. B* **83**, 195408 (**2011**).
[6] O. J. F. Martin, A. Dereux, and C. Girard, *J. Opt. Soc. Am. A*, **11**, 1073–1080 (**1994**).
[7] P. B. Johnson and R. W. Christy, *Phys. Rev. B*, **6**, 4370–4379 (**1972**).
[8] E. Palik, G. Ghosh, *Academic Press: New York*, **3**, (**1997**).
[9] Xiaofeng Li, Nicholas P. Hylton, Vincenzo Giannini, Kan-Hua Lee, Ned J. Ekins-Daukes and Stefan A. Maier; Progress in Photovoltaics: Research and Applications, **21**, 109–120, (**2013**).